Supporting Information

Mercury speciation based on mercury-stimulated peroxidase mimetic activity of gold nanoparticles

Jian-Yu Yang†, Xin-Di Jia†, Xiao-Yan Wang, Ming-Li Chen, Ting Yang*, Jian-Hua Wang

Research Center for Analytical Sciences, Department of Chemistry, College of Sciences, Box 332, Northeastern University, Shenyang 110819, China

Corresponding Author

*E-mail: yangting@mail.neu.edu.cn (T. Yang);

Tel: +86 24 83688944; Fax: +86 24 83687659

†These authors contributed equally.

Table of contents

Experimental details

Materials and Chemicals. Standard stock solutions of mercury (GSB 04-1728-2004), methylmercury (GSB 08675), and Ethylmercury (GBW(E)081524) and the human hair (GBW070601a) were obtained from the National Institute of Metrology (Beijing, China). Chloroauric acid hydrate ($HAuCl_4 \cdot 4H_2O$), polyvinyl pyrrolidone (PVP-30), anionic and metal ion salts were obtained from Sinopharm Chemical Reagent Co. (Beijing, China). All the reagents were used as received without further purification. Ultrapure water of 18.2 MΩ·cm was used to prepare all the solutions. The fish samples were acquired from the local supermarket (Shenyang, China).

Apparatus. UV−vis absorption spectra were recorded on a U-3900 UV−vis spectrophotometer (Hitachi High-Technologies Corporation, Japan). TEM image of PVP-AuNPs was acquired on a G20 transmission electron microscope (FEI Ltd., USA) at an accelerate voltage of 200 kV. The hydrodynamic diameters and the zeta potential of PVP-AuNPs were acquired from Malvern Nano ZS90 nanosizer in citrate buffer (pH 5.0, 25 mM) at 25 °C (Malvern Instruments Ltd., England). The XPS spectra of AuNPs were recorded on an ESCALAB 250 X-ray photoelectron spectrometer (Thermo Instruments Inc.).

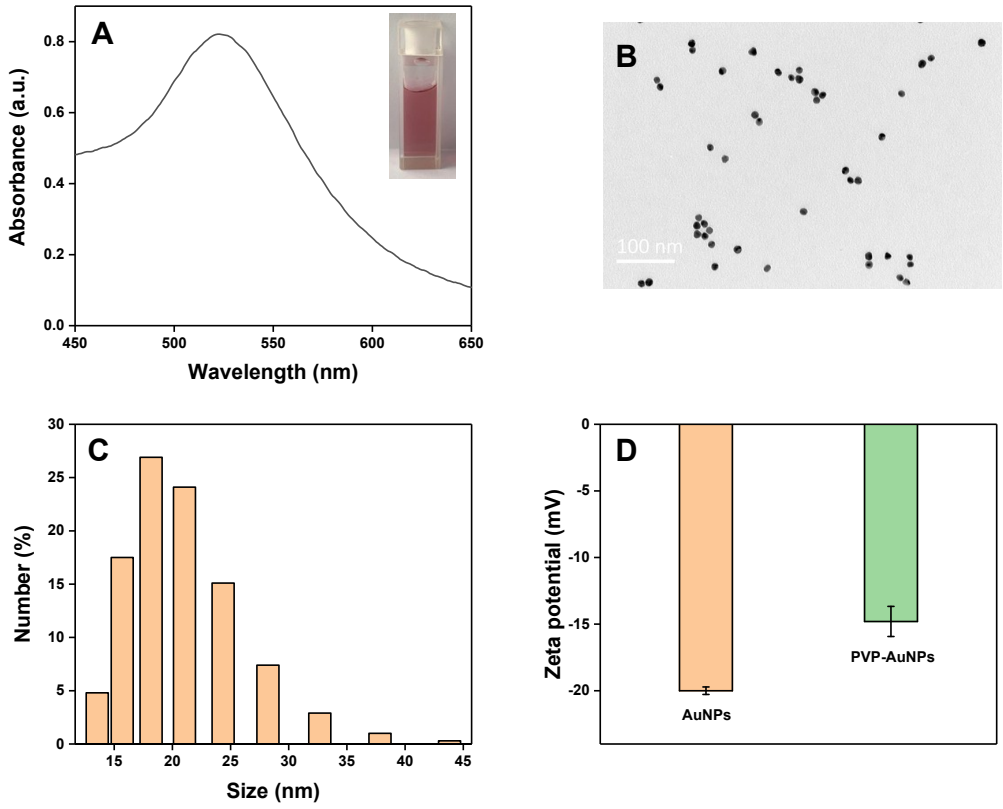

Fig. S1 (A) UV-vis absorption spectrum of PVP-AuNPs, the insert showed a photograph of PVP-AuNPs under sun-light. (B) TEM image of PVP-AuNPs. (C) The hydrodynamic diameter of PVP-AuNPs. (D) Zeta potential of AuNPs and PVP-AuNPs in citrate buffer solution (pH 5.0, 25 mM).

The PVP-AuNPs exhibited a strong surface plasmon resonance at 519 nm, causing wine-red color in visible light (Figure S1A). The distribution and size of PVP-AuNPs was investigated by TEM. As shown in Figure S1B, the PVP-AuNPs displayed good dispersion and uniform structure. The average size of these particles was measured to be about 13 nm. The hydrodynamic diameter of the PVP-AuNPs estimated from dynamic light-scattering measurement was a little larger due to the capping of PVP on the surface of AuNPs (Figure S1C). The zeta potential of PVP-AuNPs in the citrate buffer solution (pH 5.0, 10 mM) was measured to be -15.6 mV (Figure S1D).

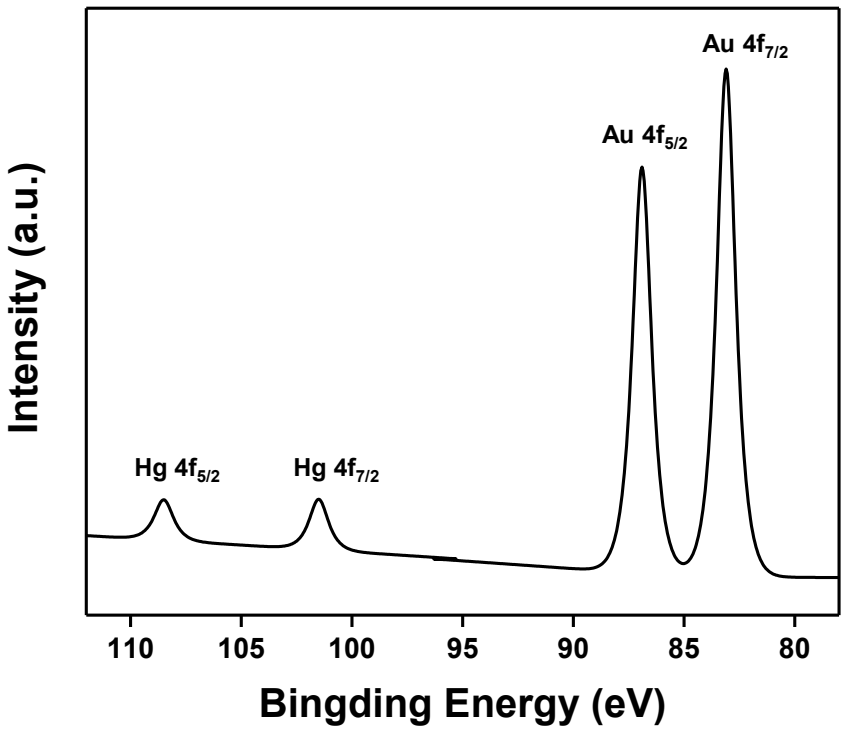

Fig. S2 XPS spectrum of PVP-AuNPs in the presence of 1 μM Hg^{2+}.

XPS measurements were used to verify the presence of mercury on the surface of PVP-AuNPs after incubation with Hg^{2+}. We could estimate the oxidation of Au and Hg by measuring the position of their $4f_{7/2}$ components. The binding energy of Au $4f_{7/2}$ and Hg $4f_{7/2}$ after incubation with Hg^{2+} were observed at 83.2 and 101.0 eV, suggesting that both gold and mercury were present in the form of metallic state in the sample.[1-2] The atomic ratio of Au:Hg in the AuNPs/Hg^{2+} system was calculated to be 90.5:9.5 by comparing their Hg and Au peak areas. The data suggested that the surface of PVP-AuNPs contains metallic mercury after incubation with Hg^{2+}.

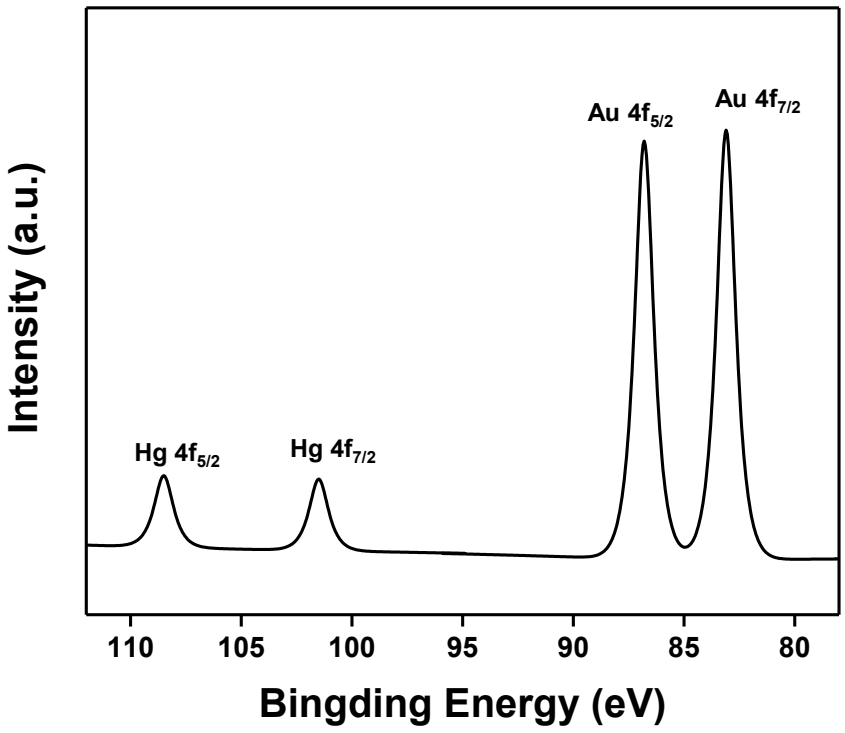

Fig. S3 XPS spectrum of PVP-AuNPs in the presence of 1 μM CH_3Hg^+.

The XPS measurements were used to verify the presence of mercury on the surface of PVP-AuNPs after incubation with $CH_3Hg^+/NaBH_4$. The binding energy of Au $4f_{7/2}$ and Hg $4f_{7/2}$ after incubation $CH_3Hg^+/NaBH_4$ were observed at 83.2 and 101.0 eV, suggesting that both gold and mercury were present in the form of metallic state in the sample.[1-2] The atomic ratio of Au:Hg in the AuNPs/$CH_3Hg^+/NaBH_4$ system was calculated to be 85.7:14.3 by comparing their Hg and Au peak areas. The data suggested that the surface of PVP-AuNPs contains metallic mercury after incubation with $CH_3Hg^+/NaBH_4$.

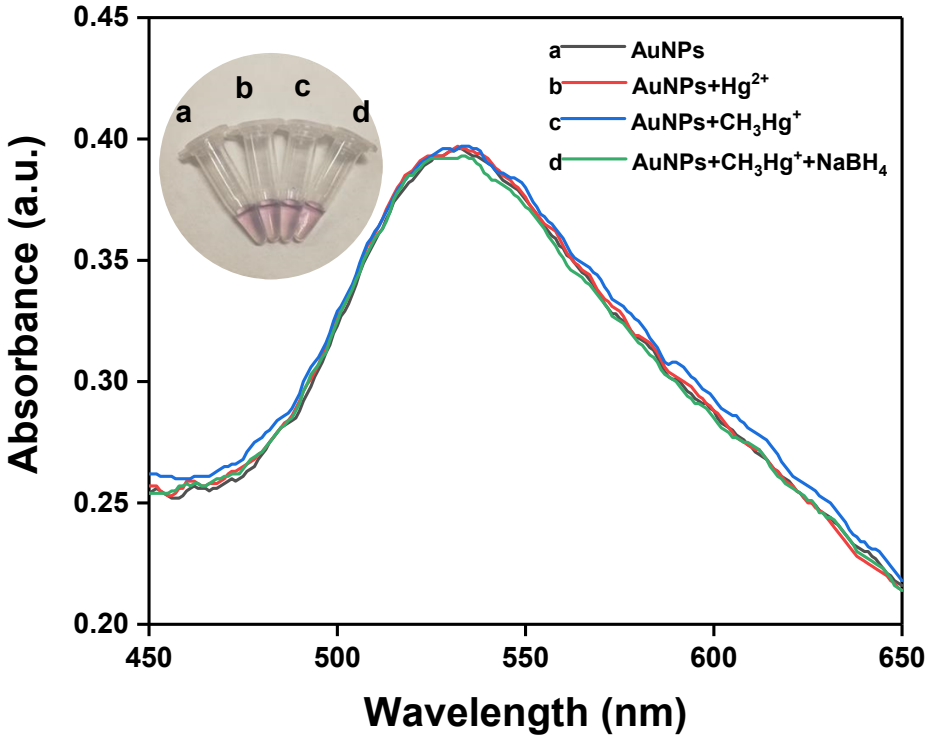

Fig. S4 (A) UV-vis absorption spectra of PVP-AuNPs in the absence and presence of Hg^{2+}, CH_3Hg^+ and $CH_3Hg^+/NaBH_4$ in citrate buffer solution (pH 5.0, 25 mM), the inset showed the images of the corresponding PVP-AuNPs. The concentrations of Hg^{2+} and CH_3Hg^+ were both 1 μM.

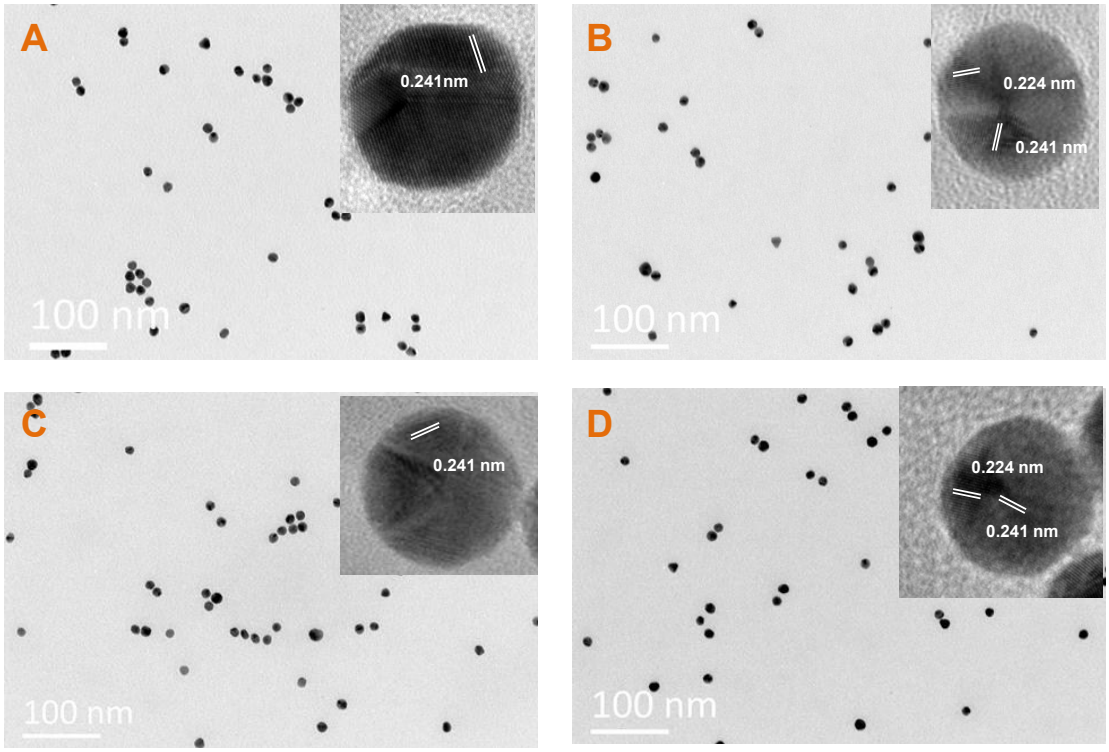

Fig. S5 TEM image of (A) PVP-AuNPs, (B) PVP-AuNPs in the presence of 1 μM Hg^{2+}, (C) PVP-AuNPs in the presence of 1 μM CH_3Hg^+, (D) PVP-AuNPs in the presence of 1 μM CH_3Hg^+ after addition of $NaBH_4$.

The average size of PVP-AuNPs was measured to be 12.7 nm (Figure S5A). The core size of PVP-AuNPs was increased to 15.2 nm (Figure S5B) or 14.9 nm (Figure S5D) after the addition of Hg^{2+} or $CH_3Hg^+/NaBH_4$. However, the core size of PVP-AuNPs did not change significantly after the addition of CH_3Hg^+ alone.

In addition, the inter-planar spacing of 0.24 nm corresponds to Au (111) planes of the face-centered cubic phase.[3] Furthermore, the lattice values of 0.223 nm relates to the typical (111) plane of Au_3Hg amalgam, which indicated the formation of Au-Hg thin amalgam layer on the surface of PVP-AuNPs.[4]

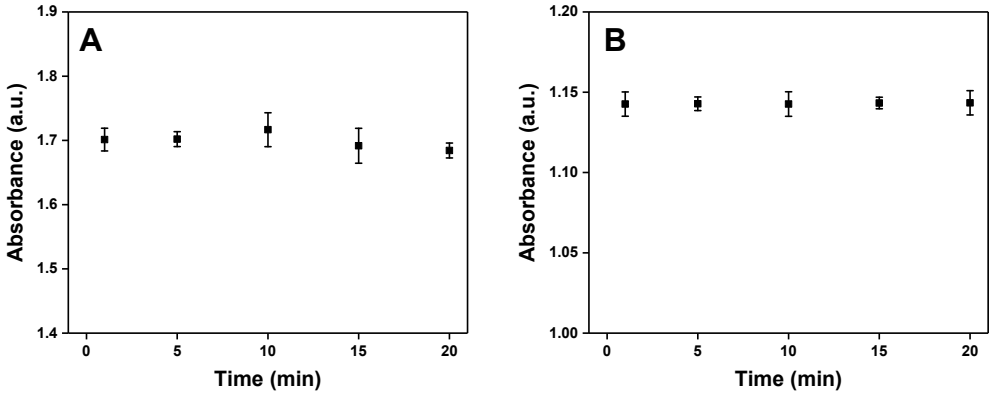

Fig.S6 The effect of incubation time between Hg^{2+} (1 μM) and citrate (A) or between CH_3Hg^+ (1 μM) (B) and $NaBH_4$ on the absorbance of the sensing system.

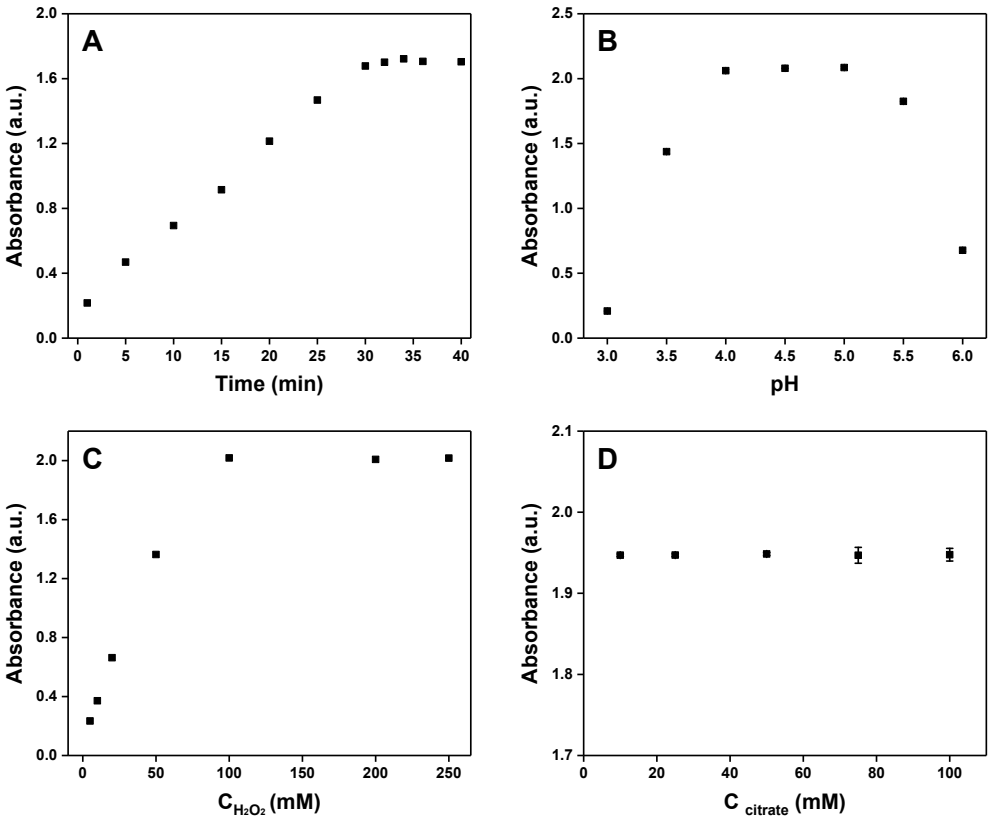

Fig. S7 The effect of (A) incubation time, (B) pH, (C) the concentration of H_2O_2 and (D) the concentration of citrate in buffer solution on the absorbance of the sensing system.

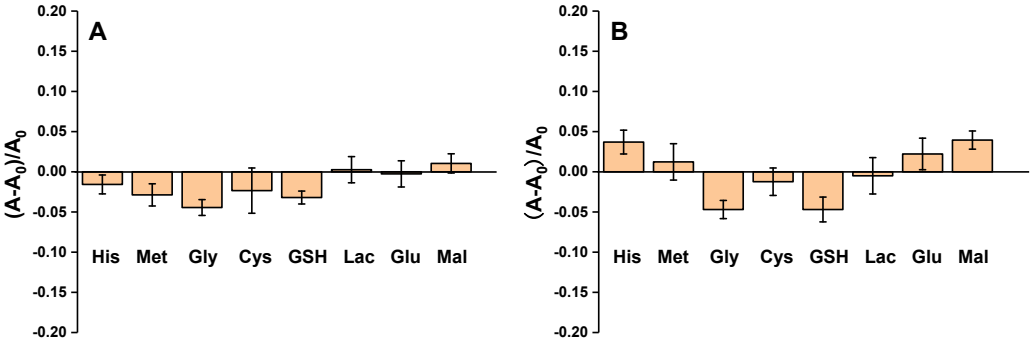

Fig. S8 (A) Effects of amino acid and carbohydrate on the peroxidase-like activity of PVP-AuNPs in citrate buffer solution (pH 5.0, 25 mM). (B) Effects of amino acid and carbohydrate on the peroxidase-like activity of PVP-AuNPs after addition of $NaBH_4$ (5 mM) in citrate buffer solution (pH 5.0, 25 mM). The concentration of histidine (His), methionine (Met), glycine (Gly), glucose (Glu), lactose (Lac) and maltose (Mal) is 1 mM, the concentration of glutathione (GSH) is 0.05 mM and the concentration of cysteine (Cys) is 0.1 mM.

Table S1. Comparison of the proposed approach with other reported methods for the detection of inorganic mercury or organic mercury based on AuNPs.

Probe	Target	Linear range	LOD	Real sample	Mercury speciation	Ref.
H_2O_2-TMB-AuNPs (mimic enzyme)	Hg^{2+}	1-600 nM	0.3 nM	Lake water	x	5
4-nitrophenol-$NaBH_4$ -AuNPs (mimic enzyme)	Hg^{2+}	5-1000 nM	1.45 nM	Tap water	x	6
rhodamine B-$NaBH_4$ -AuNPs (mimic enzyme)	Hg^{2+}	1-600 nM	2.54 nM	Waste water	x	7
formic acid-AuNPs (SPR)	$MeHg^{+}$		0.2 μM		x	8
DNA-Templated Alloy Ag−Au NPs (SPR)	$MeHg^{+}$ $EtHg^{+}$	0.0-200 μM 0.0-200 μM	0.5 μM 0.6 μM	Fish Muscle	√	9
thymine-based ligand-AuNPs (SPR)	Hg^{2+} CH_3Hg^{+}	20–80 μM 0–370 μM	15 μM 1.7 μM		√	10
Diethyldithiocarbamate -AuNPs (SPR)	Hg^{2+} $MeHg^{+}$ $EtHg^{+}$ $PhHg^{+}$	10 nM-0.1 μM 0.015-0.8 μM 0.026-1.3 μM 0.15-1.20 μM	2.9 nM 2.6 nM 8.5 nM 30 nM	Drinking water	√	11
This work (mimic enzyme)	Hg^{2+} $MeHg^{+}$, $EtHg^{+}$	5-100 nM 5-100 nM	1.9 nM 0.9 nM	Hair Fish	√	

Reference

(1). A. Singh, R. Pasricha and M. Sastry, *Analyst* **2012,** 137 (13), 3083-3090.

(2). S. K. Das, C. Dickinson, F. Lafir, D. F. Brougham and E. Marsili, Synthesis, *Green Chem.* **2012,** 14 (5), 1322-1334.

(3). Z. Yin, B. Chen; M. Bosman, X. Cao, J. Chen and B. Zheng; H. Zhang, *Small* **2014,** 10 (17), 3537-43.

(4). I. Ojea-Jiménez, X. n. López, J. Arbiol and V. Puntes, *ACS Nano* **2012,** 6 (3), 2253-2260.

(5) Y. J. Long, Y. F. Li, Y. Liu, J. J. Zheng, J. Tang and C. Z. Huang, *Chem. Commun.*, 2011, **47**, 11939-11941.

(6) Z. Chen, C. Zhang, Q. Gao, G. Wang, L. Tan and Q. Liao, *Anal. Chem.*, 2015, **87**, 10963-10968.

(7) G. Chen, J. Hai, H. Wang, W. Liu, F. Chen and B. Wang, *Nanoscale*, 2017,9, 3315-3321.

(8) P. Donati, M. Moglianetti, M. Veronesi, M. Prato, G. Tatulli, T. Bandiera and P. P. Pompa, *Angew. Chem. Int. Ed.*, 2019, 58, 1–6.

(9) Z. Chen, X. Wang, X. Cheng, W. Yang, Y. Wu and F. Fu, *Anal. Chem.*, 2018, **90**, 5489-5495.

(10) M. L. Aulsebrook, E. Watkins, M. R. Grace, B. Graham and K. L. Tuck, *ChemistrySelect*, 2018, **3**, 2088-2091.

(11) L. Chen, J. Li and L. Chen, *ACS Appl. Mater. Interfaces*, 2014, **6**, 15897-15904.